Proceedings of the Seventh International Conference on
Railway Technology: Research, Development and Maintenance
Edited by: J. Pombo
Civil-Comp Conferences, Volume 15, Paper 18.13
Civil-Comp Press, Edinburgh, United Kingdom, 2026
ISSN: 2753-3239, doi: 10.4203/ccc.15.18.13

Development of a Lateral Displacement Mechanism for a Single Wheel Roller Rig

J. Goersch, J. Wagner, N. Jaeger and R. Pfaff

Institute for Rail Vehicles (IFS), RWTH Aachen University, Germany

Abstract

This paper describes the design and initial testing of a lateral movement unit implemented on a single wheel roller rig. The unit was installed in the single wheel roller rig (swr) in use at the Institute for Railway Vehicles (ifs) at RWTH Aachen University. Wheelsets start to oscillate in lateral direction when operated, generally known as hunting oscillation. Because of the lateral movement, the wheels surface area in contact with the rail is exposed to changing mechanical stress situations during operation. While the typical hunting oscillation of a railway wheelset can be witnessed on a single axle roller rig, it cannot be observed on a single wheel roller rig. To simulate realistic conditions on a single wheel roller rig, the lateral movement must be artificially generated. This paper proposes a design to incorporate an oscillation mechanism into the existing swr at ifs considering existing boundary conditions. In addition, an extension for a wide range of wheel diameters in between 600 to 1000 mm is presented.

Keywords: wheel-rail contact, hunting oscillation, lateral wheel displacement, lateral force, roller rig, design.

1 Introduction

Testing changes in wheel profile geometry or new materials usually is not carried out directly in the real vehicle, as rail vehicle wheels are critical regarding safety and any failure can lead to catastrophic results. Therefore, such tests are usually carried out on test benches where test parameters can be independently defined and monitored in detail. Roller rigs provide a controllable and safe test environment with repeatable conditions. It can also be used to test designs that have not yet been approved for field testing. The necessary evidence for approval can be provided by means of suitable tests. In this area, operational tests on a roller rig are (still) superior to mathematical simulations [1]. Furthermore, test benches offer considerable time savings in conducting tests utilizing the time-lapse effect where wear and damages to wheel and roller can be created in much shorter running distances [1], [2]. Limitations of roller rigs include the smaller size of the contact patch which is decreasing with decreasing diameter of the roller in comparison to the wheel [2].

1.1 Roller rigs

Roller rigs are commonly used for tests in wheel-rail contact research, research on wear and tests with new wheel(set) designs. Three main designs, a single wheel roller rig, wheelset or bogie test benches are mainly used. A roller (or a pair of rollers) is shaped according to the selected rail profile and provides the rail for the vehicle wheel to be tested on. The roller usually includes the rail inclination with a value of 1:40 or 1:20 to keep simulation as close to reality as possible. Single wheel roller rigs consist of a single pair of wheel and roller whereas wheelset roller rigs can conduct tests with complete wheelsets and bogie test benches of a complete bogie incorporating multiple wheelsets.

Single wheel roller rigs are usually utilized for research into wear and rolling contact fatigue processes, for experiments with friction coefficient modifications, acoustic tests and for testing new rail materials [3]. Single wheelset roller rigs are used for research into braking performance, crack propagation tests on wheelset axles and new wheelset designs. [4], [5]

Examples of roller rigs are Knorr-Bremse's wheelset roller rig in Munich, Germany with a drive power of $1400\ kW$, the roller rig of Lucchini RS in Lovere, Italy with a drive power of $500\ kW$, and CARS' roller rig in Beijing, China with $2400\ kW$ of drive power. Some other roller rigs and their technical specifications can be found in [6]. For comparison, the single wheel roller rig at ifs offers $75\ kW$ drive power. The current design of this roller rig will be explained in the following section.

1.2 Current roller rig design

The single wheel roller rig at ifs consists of a roller, representing the rail and the (vehicle) wheel, which is usually the test specimen. When in use, the roller (number 1 in Figure 1) powered by the electric motor (3) starts to spin, which drives the specimen wheel (2) due to friction in the contact area. This contact area represents the wheel-rail contact in real applications. Loads of up to $10\ t$ can be applied by a rubber air suspension (4) filled with compressed air. Braking with a controllable anti-slip system is realized by a disc brake (5). This also enables the system to create conditions of high wheel slip at braking.

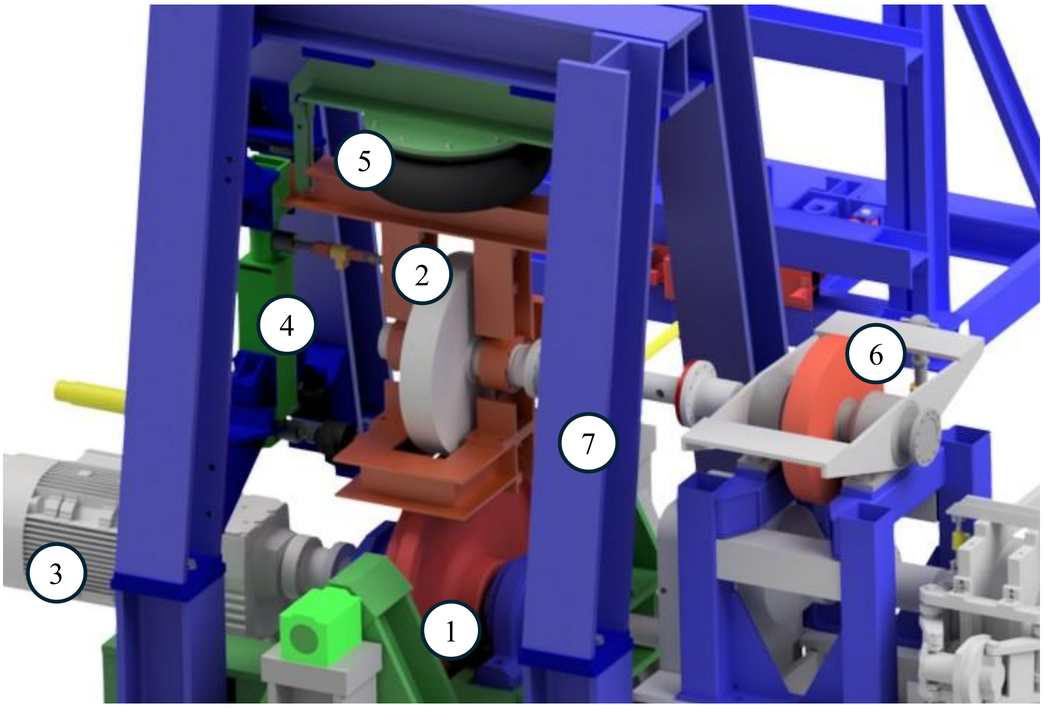

1	roller	5	air spring
2	specimen wheel / railway vehicle wheel	6	disc brake
3	asynchronous motor	7	mounting frame
4	lateral displacement guiding assembly		

Figure 1: CAD representation of the single wheel roller rig at ifs

1.3 Wheel-rail contact forces

Since a wheelset has two wheel-rail contact points and the tread profiles are mirrored, the lateral component S_γ cancel each other, as shown in Figure 2. Therefore, a roller rig with a wheelset does mainly need to transfer forces in longitudinal direction. The single wheel contact in the swr produces a force that needs to be compensated through the structure of the roller rig. This force is called geometric lateral wheel force S_γ and its value is linear dependent from the cone angle in the contact point and the load on the wheel, see equation *(1)*. [7]

$$S_\gamma = Q \cdot \tan\gamma \tag{1}$$

$$N = \frac{Q}{\cos\gamma} \tag{2}$$

In z direction, masses and the applied loads result in a normal force that is transferred into the rail. Its value can be calculated using equation (*2*).

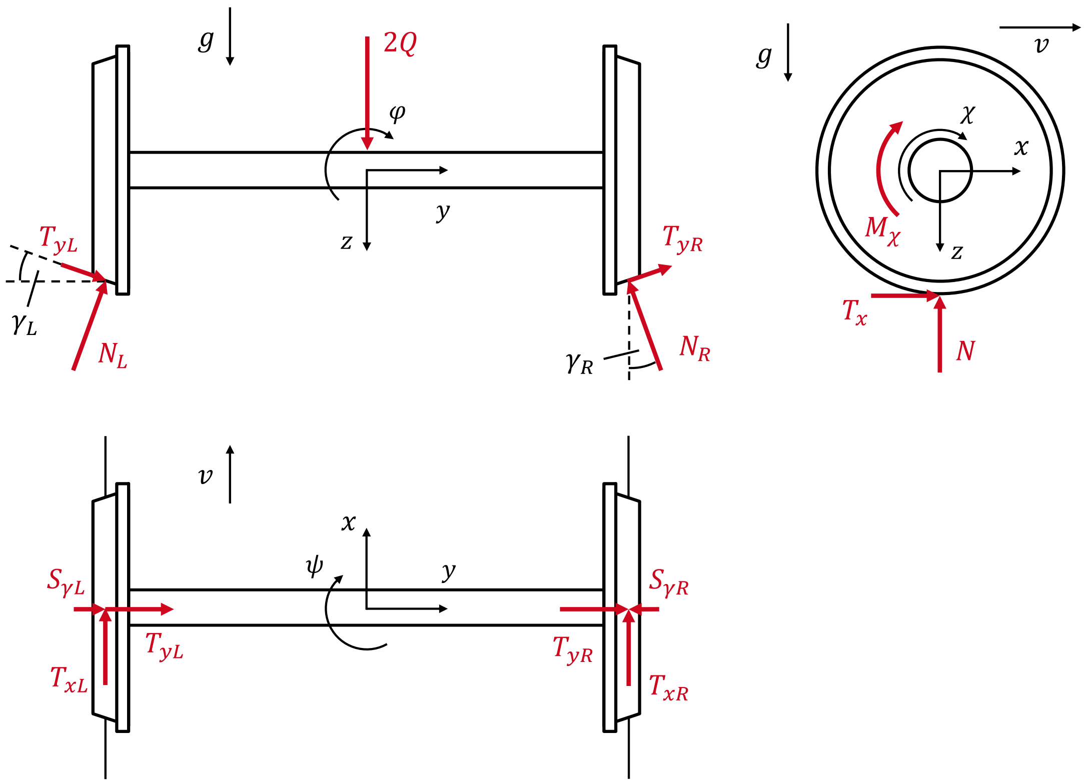

Figure 2: Wheelset in space with acting wheel-rail contact forces, based on [7]

When running a wheelset, the position of the wheels might change from the perfectly centered position as seen in Figure 1. When the wheelset is displaced by a value of Δy, the geometric lateral forces change values and no longer cancel out. The resulting lateral force pushes the wheelset into center track direction. Additionally, the displacement causes one wheel to run on a larger diameter, causing the wheelset to turn around its z-axis. Running in this position creates lateral slip s_y, and therefore a lateral creep force T_y, which can be calculated using equation *(3).* [7]

$$T_y = -f_y \cdot Q \cdot \frac{s_y}{|s_y|} \tag{3}$$

When the wheelset reaches the track center, geometric lateral forces again cancel out. Since the wheelset is still turned in ψ and therefore laterally slipping, lateral adhesion forces push the wheelset further to the opposite rail. Leaving the center of the track, a resulting geometric lateral force builds up again and eventually stops the wheelset from further shifting. Now the opposite wheel runs on a greater diameter, causing the process to repeat in opposite direction. This movement along the track is known as hunting oscillation and can be observed when a running wheelset is displaced by Δy or rotated by $\Delta\psi$ in the track. The oscillation in y-direction is dependent to the driving speed v and the equation of motion can be written as $\ddot{y} + \Omega^2 y = 0$. Solving the equation of motion for a cone shaped wheel, one will get the following equation (*4*) for the displacement in lateral direction, where L is the nominal radius of the wheel in center position: [7]

$$y{=}y_0\cdot \cos \Omega t = y_0 \cdot \cos \frac{2\pi}{L} vt \tag{4}$$

Whereas the angular motion can be described with the following equation [7]:

$$\psi{=}\frac{\dot{y}}{v} = -\frac{2\pi}{L} \sin \Omega t \tag{5}$$

While the forces create hunting oscillation, they also ensure self-centering and track guidance of the wheelset. These movements only occur on a wheelset, where the motion of both wheels is coupled and forces are transferred between wheels [7]. When operating a single wheel, running on a larger diameter does not create a rotation in ψ, and no equilibrium of geometrical forces exist. Thus, running a single wheel roller rig comes with additional requirements to conduct forces and constrain degrees of freedom.

1.4 Degrees of freedom

A single wheel in space has six degrees of freedom, that are shown in Figure 2. By reducing a wheelset to a single wheel, it loses the track guidance ability. Structural improvements must be applied to constrain the degrees of freedom and retain the wheel in position. In the current structure of the swr, the frame of the single wheel constrains four degrees of freedom: Any movement along the x-axis is constrained due to three long rods which are connected to an outer ballast. As the rods are connected to the outer ends of the wheels frame, they also constrain the rotation around the z-axis, which represents the angle of attack ψ. In y-direction, the frame is connected to a lateral guiding assembly via rods which is held in place with a hydraulic actuator for manual lateral displacement. Rotation around the x-axis is constrained by linear bearings. Displacement in the z-axis is constrained by the contact between wheel and roller. The rotational freedom of the wheel around the y-axis is not constrained as it represents the driving rotation.

Thus, the swr currently only allows manual lateral displacement via the hydraulic actuator and hunting oscillation as described before is constrained. The redesign aims to integrate a cyclical lateral excitation to introduce hunting oscillation and therefore create more realistic load characteristics. In addition, the redesign aims to fit wheels of diameters larger than $671\ mm$ into the test bench.

2 Re-Design of the Roller Rig

As previously introduced, the setup of the roller rig at ifs in its current design only supports testing of wheels with a diameter of up to $671\ mm$. To enable the ifs to test freight wagon wheels, that usually have diameters greater than $671\ mm$, the roller rig must be adapted. At the same time the roller rig should still be able to house smaller wheels to enable usage for a variety of projects with different wheel sizes. Therefore, a solution for simple integration of variable diameter of wheel sizes into the test bench is necessary. The second constraint consists of the existing main mounting frame of the roller rig which should remain unchanged to maintain feasibility in terms of time and funding of the project.

As described in the previous section, the current roller rig setup can apply longitudinal forces (T_x) resulting from the powered roller and the implementation of a brake with slip control on the wheel axis. Normal forces can be applied by the existing air spring. Lateral forces (T_y) are currently constrained, which is identified as a major gap to emulate field conditions. From this analysis of test cases key requirements for the test bench result to:

- Integrating of a variable mounting frame for wheel diameters between 534 and 1000 mm;
- Keeping functionality of the current design;
- Integrating of a degree of freedom for lateral displacement of the wheel during experiments;
- Overcoming design challenges within the given geometric and spatial constraints (e.g. keeping the main mounting frame unchanged)

2.1 Variable mounting frame

Several design iterations were conducted to apply a simple and cost-efficient solution to a mounting frame for the required wheel diameters. Solutions with an adjustable frame such as a spindle lift system, a pneumatic system and a rack and pinion mechanism have been studied in [8] but were discarded due to their cost, complexity and uncertainty in long term reliability. Therefore, a frame with adapters of different sizes which will be mounted depending on the wheel diameter, was selected. In combination with the air spring, which enables a vertical displacement wheel diameters from 534 to 1000 mm, the system can be integrated into the frame using two different frame-adapter sizes, as shown in Figure 3.

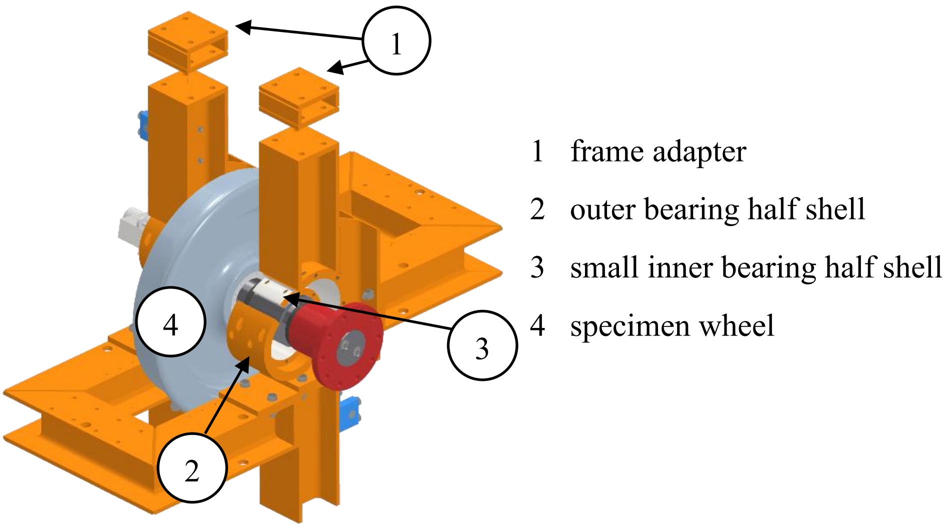

Figure 3: Partly exploded view of variable mounting frame with adapter and bearing half shells

Different axles are required, as the resulting torque increases with increasing wheel diameter and the central hub of the wheels have different diameters. This results in two required bearing sizes, which are incorporated into the redeveloped frame by altering the bearing half shell.

2.2 Lateral displacement

The current setup only allows a fixed lateral displacement between wheel and roller to be set before the start of the experiment by utilizing the manually operated hydraulic actuator described in Section 1.4. An enhancement to better emulate the behavior of a wheelset in the field is to integrate a lateral displacement mechanism, which dynamically adjusts the wheels lateral position to emulate real world hunting oscillation of the wheelset [7].

As the single wheel roller rig only consists of a single wheel, a lateral displacement mechanism needs to provide forces of the missing wheel. The lateral force is dependent on the wheel profile angle as shown in equation (*1*). Because flange contact during normal operation only occurs in tight curves and in driving over switches, flange contact situations are not considered and the maximum wheel profile inclination γ is therefore approximated to $10°$. The force required to move the wheel is direction-dependent and is composed of three main contributions:

1. Geometric force arising from the wheel-rail geometry S_{γ},
2. Friction forces – both static and dynamic – acting between the wheel and the rail, and
3. Friction of lateral-displacement guiding assembly (lga) (Figure 1; 4), which uses linear recirculating-ball bearing units.

In addition, an acceleration force F_a caused by the lateral displacement has to be considered. Consequently, the total required force is obtained from the equation given below.

$$F = S_{\gamma} + F_{S,W} + F_{D,W} + F_{S,lga} + F_{D,lga} + F_a \tag{6}$$

with

$$F_S = \mu_S \cdot m$$
$$F_D = \mu_D \cdot m$$
$$F_a = m \cdot a_y$$
$$a_y = 4A \cdot (\pi \cdot f)^2 \cdot \cos(2\pi \cdot f \cdot t)$$

With equation (*6*) the resulting maximum force for the lateral displacement results to $72\ kN$ and the average force in one cycle results to $50\ kN$. The calculation parameters such as constants and the assumed frequency and amplitude of the sinus movement are displayed in Table 1.

Table 1: Calculation Parameters

Parameter	Description	Value
μ_S	Static friction coefficient	0.4
μ_D	Dynamic friction coefficient	0.1
m [kg]	Wheel load	11,250
γ [°]	Wheel profile inclination	10
f [Hz]	Frequency of sinus oscillation	5
A [mm]	Amplitude of sinus oscillation	1

Hydraulic and electric actuators were examined as possible solutions for dynamic motion. According to common design practices (VDI 2221) [9] a ball-screw spindle combined with an electric motor was selected because it can be integrated easily into the main PLC of the test bench and requires considerably less maintenance than a hydraulic system comprising a pump, actuator, reservoir and tubing [10].

The assembly of spindle, bearing and geared electric motor is mounted to the existing lateral displacement guiding assembly. The mounting height was determined by the flow of forces between wheel-roller-contact and the lateral displacement guiding assembly. The final design is shown in Figure 4.

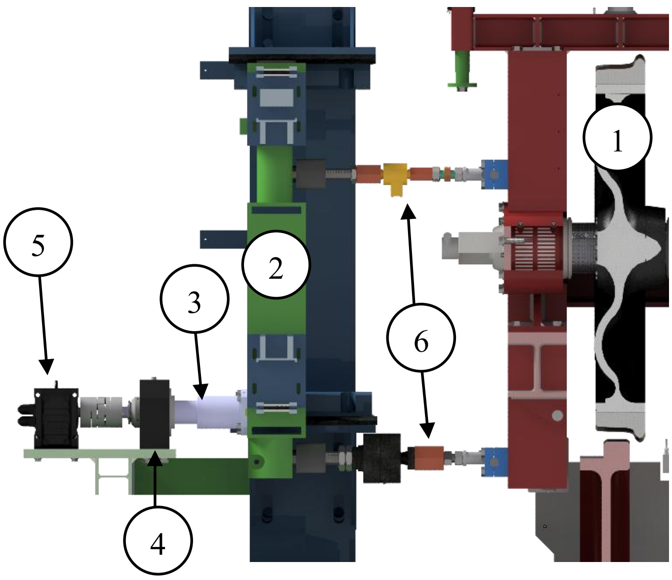

1 specimen wheel
2 lateral displacement guiding assembly
3 spindle
4 bearing
5 geared electric motor
6 connecting rods

Figure 4: Lateral displacement mechanism (cross section view of roller rig)

3 Initial testing

First tests were carried out applying slow vehicle velocity and low loads. In Figure 5 the movement of the motor and the measured lateral force in the rods connecting the guiding assembly is shown. The system shows good results for initial testing with a low frequency of 1 Hz, an amplitude of 2 mm, wheel speed of 8 km/h and a wheel load of 5 kN. Measured peak lateral force results to 5 kN, which indicates an overhead for tests with higher loads and speeds as designed.

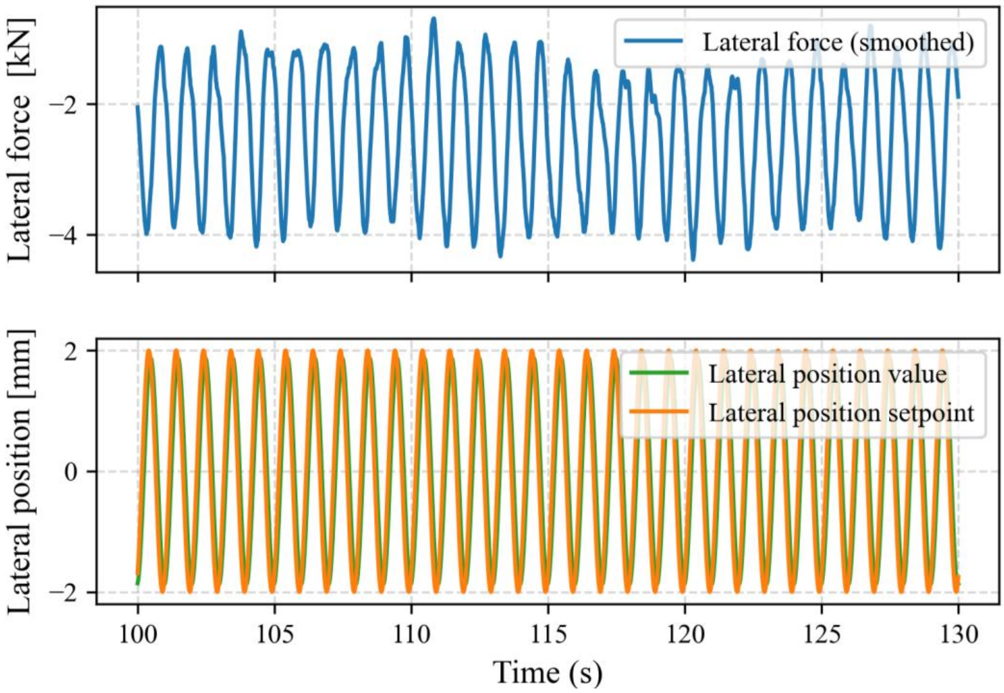

Figure 5: Lateral force and position data from roller rig

4 Conclusions and Contributions

The integration of a new mounting frame enables mounting wheels of diameters between 534 and 1000 mm. Therefore, tests with freight wagon wheels are possible. As the diameter ratio between roller and wheel shrinks with growing wheel diameter the resulting contact patch and contact situation is less comparable to field conditions. A larger diameter roller would improve the contact patch.

The first tests of the lateral displacement system show good results and the system worked as envisioned. The dynamic actuation via software enables dynamic lateral displacement of the wheel. Tests up to the envisioned frequency and amplitude in correlation with wheel loads of up to 11.25 t will be executed in the near future to test the systems overall capabilities and stability. To fully represent field conditions of the hunting oscillation, the rotation in ψ is missing.

The development of a software extension to correlate wheel speed and frequency and amplitude of the sinusoidal movement seems promising. In upcoming tests, the roller rig will be utilized to test technical alterations made to the wheel material. The lateral displacement system therefore enables tests that represent the field conditions more accurately.

Concerning test bench extension for testing technical alterations and creating more realistic test conditions, the implementation of a clasp brake would allow for more varied test scenarios and enable more realistic tests of freight wagon wheels.

Acknowledgments

Research was conducted using grants provided by the German Federal Ministry for Economic Affairs and Energy as part of the LEDA research project (Grant number: 03EN2103B).

References

[1] K. Mädler und S. Hartmann, „Ist die Entwicklung des Radverschleißes vorhersagbar? Über Vorteile und Grenzen von Rollprüfständen“, in *19. Internationale Schienenfahrzeugtagung Dresden*, Hamburg: DVV Media Group | Eurailpress, 2023.

[2] B. Liu und S. Bruni, „Analysis of Wheel-Roller Contact and Comparison with the Wheel-Rail Case“, *Urban Rail Transit*, Bd. 1, Nr. 4, S. 215–226, Dez. 2015, doi: 10.1007/s40864-015-0028-3.

[3] R. Heyder, K. Mädler, D. Ullrich, und A. Zoll, „Simulation des Rollkontakts zwischen Rad und Schiene auf 1:1-Prüfständen - Versuchsprinzipien und Anwendungen“, in *Tagungsband Graz 2014*, Berlin: Georg Siemens Verlag, 2014.

[4] Rad/Schiene-Kontakt“. Zugegriffen: 18. März 2026. [Online]. Verfügbar unter: https://www.db-systemtechnik.de/dbst-de/assets/pruefstaende/rad-schiene-kontakt-12935418

[5] M. Heller, J. Koch, C. Burger, und A. Festel, „Reproducible Braking Distance: ATLAS.“, Knorr-Bremse Systeme für Schienenfahrzeuge. Zugegriffen: 18. März 2026. [Online]. Verfügbar unter: https://rail.knorr-bremse.com/de/de/stories/fachartikel/content-page-atlas.json

[6] J. Wagner, „Entwicklung eines Antriebs für einen Einzelrad-Rollprüfstand zur Einstellung unterschiedlicher Schlupfzustände“, Masterarbeit, RWTH Aachen University, Aachen, 2025.

[7] C. Schindler *u. a.*, Hrsg., *Handbuch Schienenfahrzeuge: Entwicklung, Produktion, Instandhaltung*, 1. Aufl. Hamburg: Eurailpress, 2014.

[8] Till Keller, „Entwicklung und Konstruktion einer modularen Radaufhängung für einen Einzelrad-Rollprüfstand“, Masterarbeit, RWTH Aachen University, Aachen, 2025.

[9] *VDI-Richtlinie 2221 Methodik zum Entwickeln und Konstruieren technischer Systeme und Produkte*, Richtlinie 2221:1993–05, Mai 1993.

[10] Karl Bendler, „Entwicklung und Konstruktion einer dynamischen Lateralverschiebung von Schienenfahrzeugrädern für einen Einzelrad-Rollprüfstand“, Masterarbeit, RWTH Aachen University, Aachen, 2025.